Optimisation of End Plates in a Rotating Domain

Hashan Mendis

October 21, 2016

Contents

1 Introduction

RMIT has a Formula-SAE team that designs a race car for the international competition. An aerodynamics package has been designed for this years car consisting of a front and rear wing. An initial analysis has already designed the profiles dimensions and angles for the rear wing using straight line analysis. The rear wing has yet to be simulated in a rotating domain to determine its efficiency and how the flow structure changes.

2 Objectives

Optimize the end plate design to reduce side force in yaw.

3 Methodology

Using ANSYS CFX the end plate designs were simulated in a straight line to evaluate downforce, drag and establish a base line.

The designs were then simulated in a rotating domain of an 8.2 m radius at 40 km/hr. The rear wing was set at at 10^o yaw angle and 1.5^o of roll, simulating the race car in an event taking a constant radius corner. In order to reduce computational time the rear wing was simulated in isolation. As wind tunnel models are not present using the current wing design a mesh study will be conducted to ensure mesh independence.

4 Pre-processing

Pre-processing set up overviews the geometry, fluid domain, mesh and set up.

4.1 Geometry

The different end plate geometry is seen below. Figure 1a refers to the initial design of a square end plate with 50 mm radius edges. Figure 1b shows the end plate with a section taken off the top. The bottom cut out was taken out to represent the actual end plate design at the request of the chief engineer.

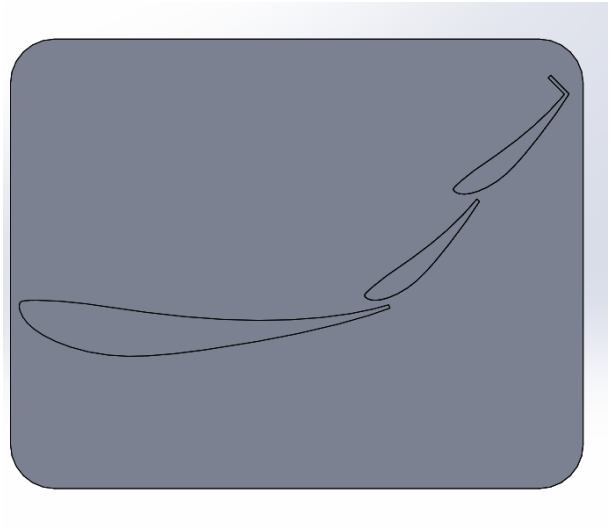

(a) Initial End Plate Geometry

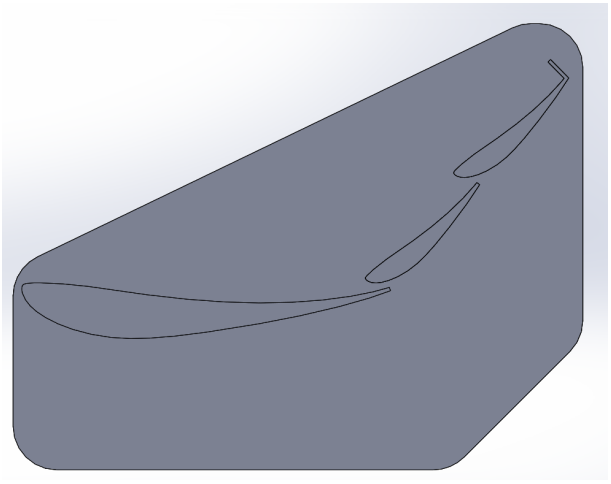

(b) Modified End Plate Geometry

Figure 1: End Plate Designs

In both situations the bottom edge of the end plate is 150 mm from the lowest point of the main element and then top edge is 30 mm from the gurney flap.

4.2 Domain

Two fluid domains were created to simulate both conditions. The rear wing were placed in a straight line to understand the flow structure and it establish a base line. The straight line domain is shown in Figure 2a
The designs were then placed a in an 8.2 m radius rotating domain at 40 km/hr as seen in Figure 2b, to understand the change in flow structure.

(a) Straight Line Domain

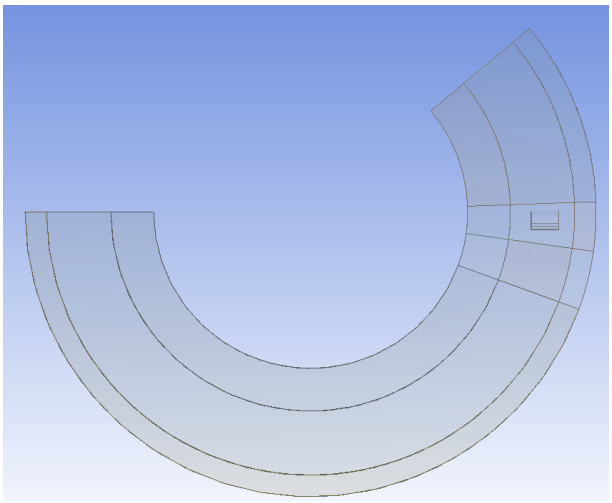

(b) Rotating Domain

Figure 2: Straight Line and Rotating Domains

A domain study was conducted to ensure the walls did not interfere with the wings and the outlet was placed far enough to resolve the wake. The results of the domain study is shown in Table 1 and used for the simulation.

Parameter	Straight Line	Rotating Domain
Outer Upwind	5 m	5 m
Outer Downwind	20 m	25 m
Outer Side	4 m	5 m
Outer Top	5 m	6 m
Inner Upwind	0.2 m	0.2 m
Inner Downwind	1.4 m	1.4 m
Inner Side	1 m	1 m
Inner Top	2 m	2 m

Table 1: Straight and Rotating Domain Dimensions

4.3 Mesh

The mesh had a tetrahedron structure as seen in Figure 3in the inner domain to conform to the complex shape, swept bias on faces touching the inner domain and hex elements used elsewhere as seen in Figure 4. The swept and hex elements would improve computational resources compared to a tetrahedron elements.[2] The bias of the swept elements downwind increased in length, dampening the swirling flow and making it easier to resolve the flow at the outlet.

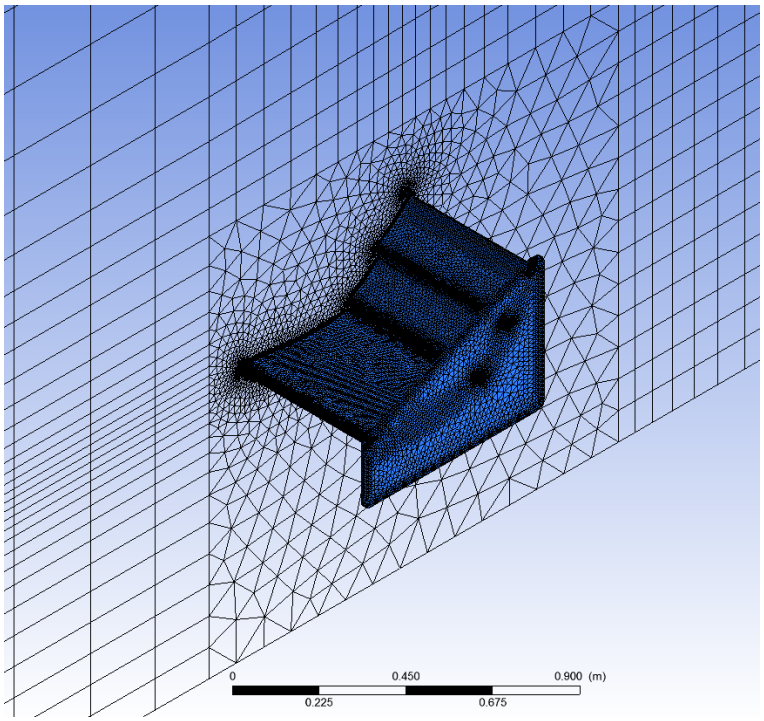

Figure 3: Surface mesh around the rear wing

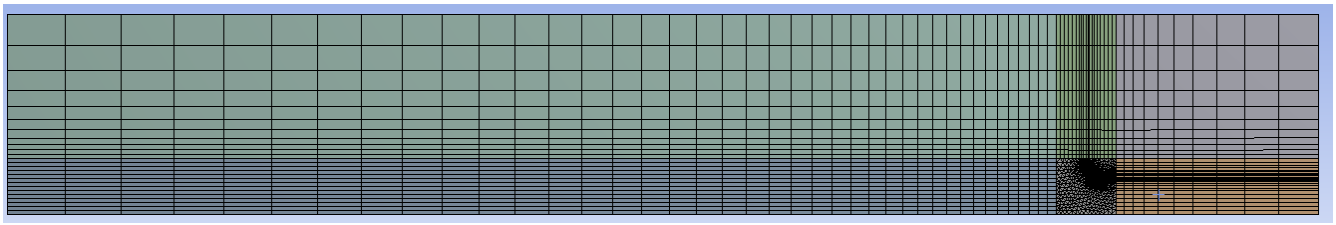

Figure 4: Swept Elements set up

Sizing controls were placed on the profile being an area of importance and on the inner volume mesh. They were also placed on small edges such as the end plates and wing trailing edges.

A mesh study was conducted on the initial end plate geometry as seen in Figure 1a to ensure the results were mesh independent. The study was conducted by halving the mesh parameters, Coefficient of lift (Cl) was monitored to ensure values were within 1%. A k-w SST turbulence model was being used and a Y+ of 1 was used for the profile to capture the boundary layer.[1]
After the volume and surface sizing was established the Y+ of the profile was studied.The Y+ was tested to determine what level of resolution is required to accurately capture the boundary layer. A Y+ 1 required 2 million elements in the inflation region, using a larger Y+ would reduce the mesh count and computational time.

The results of the mesh study in a straight line is seen in Figure 5, with data in Appendix A. The mesh study found mesh independence when the volume sizing was at 100 mm, 10 mm sizing on the profile with a first layer height of 0.01 mm, using 30 layers.

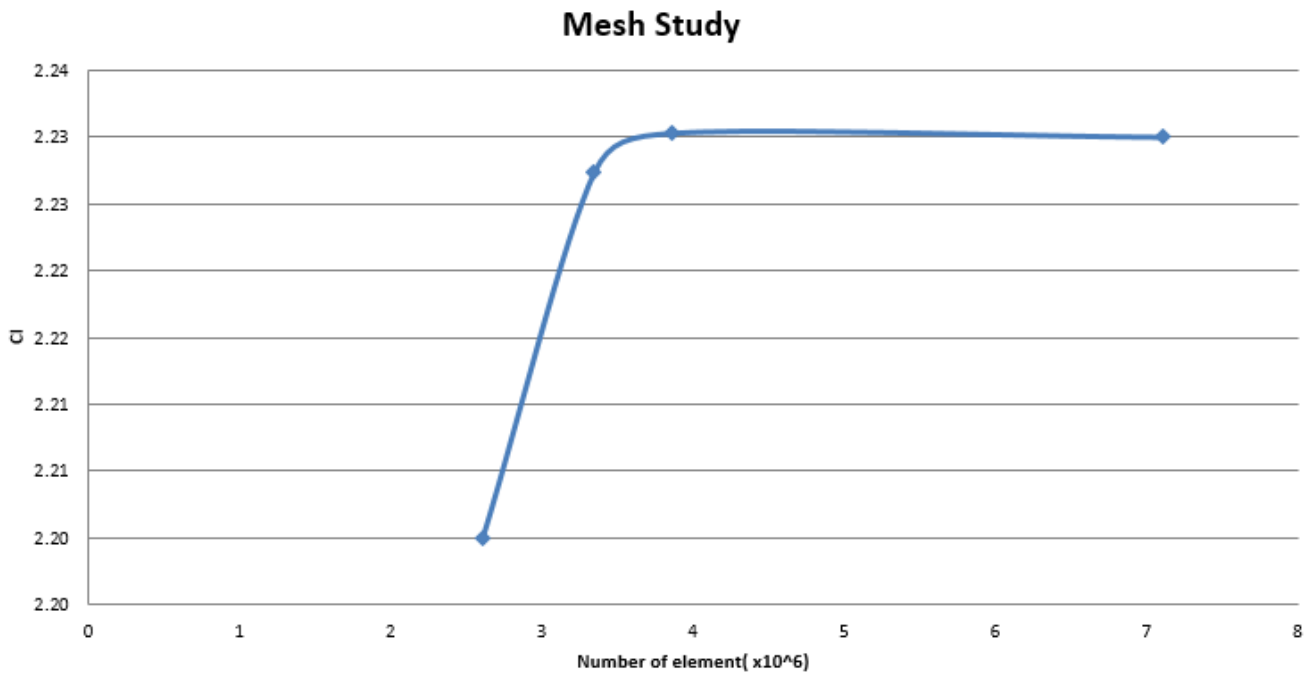

Figure 5: Mesh Study

The results of the Y+ study is shown in Appendix B, with the first layer and number of layers changed. The results show a small change in the over all Cl of the rear wing, however a flow structure change is evident.
During the study the boundary layer was checked by using the Turbulent Viscosity Ratio. It is the ratio between the turbulent viscosity and molecular viscosity . The ratio was plotted against the symmetry plane as seen in Figure 6. The model is using a Y+ of 1 with 30 layers, adjacent to the wall is the laminar sub layer, showing laminar flow resulting in no turbulence viscosity. As the flow progressed into the logarithmic region, turbulence viscosity increases in the boundary layer, then dissipating approaching the free stream. The transition is capture in the inflation layer showing the boundary layer height is appropriate. This approach was checked during the Y+ study to ensure the boundary layer is captured at all times. [3]

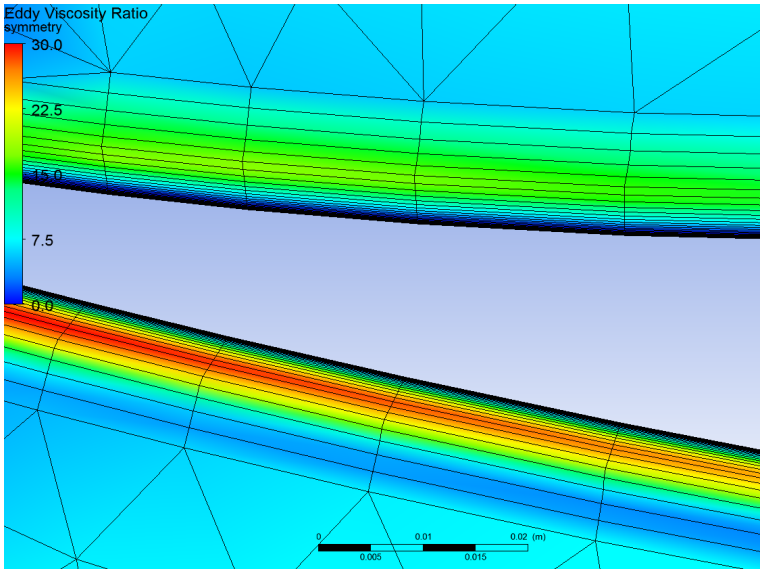

Figure 6: Turbulent Viscosity Ratio on symmetry

The velocity contour is shown in Figure 7a. It shows separation of the second element at the same place on all cases. Looking at the Turbulence Kinetic Energy (TKE) in Figure 7b, the energy of the system changes after a Y+ of 7. As the first layer height of the boundary layer increase, after a Y+ of 7 it does capture the energy within the layer. This will result in errors in the flow structure being unable to predict separation in other places.

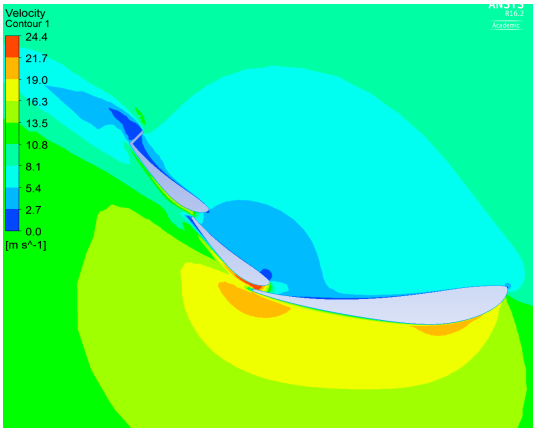

(a) Velocity on Symmetry Plane

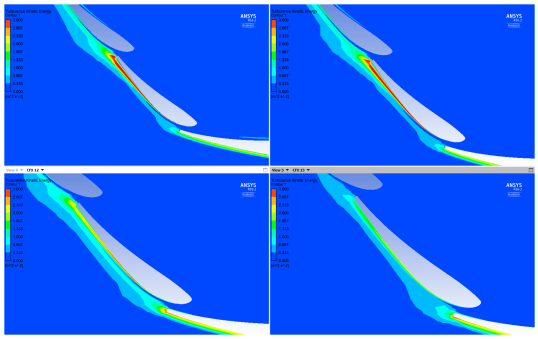

(b) Top left:Y+1,Top right:Y+7,Bottom left:Y+30,Bottom right:Y+60

Figure 7: Contour on symmetry plane

Mesh study of the rotating domain using the initial end plate design was also conducted concluding the mesh used for the straight line analysis was appropriate. As before an inner refinement zone had tetrahedron elements, local refinement around, profiles and small edges as seen in Figure 8a. The outer domain contained swept elements, increasing in length towards the outlet as seen in Figure 8b.

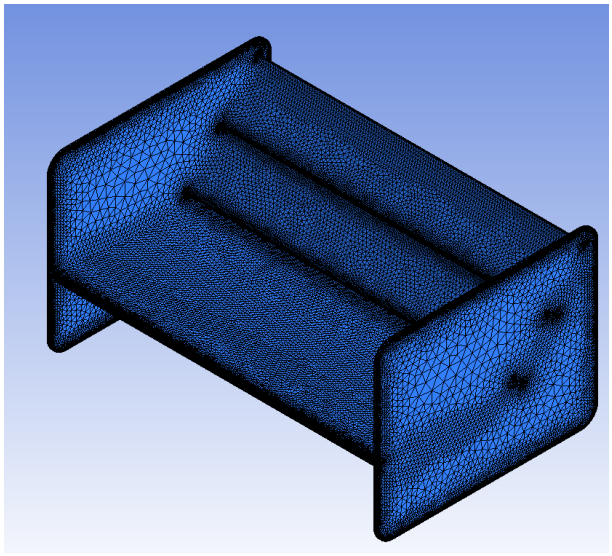

(a) Surface mesh of the wing in the rotating domain

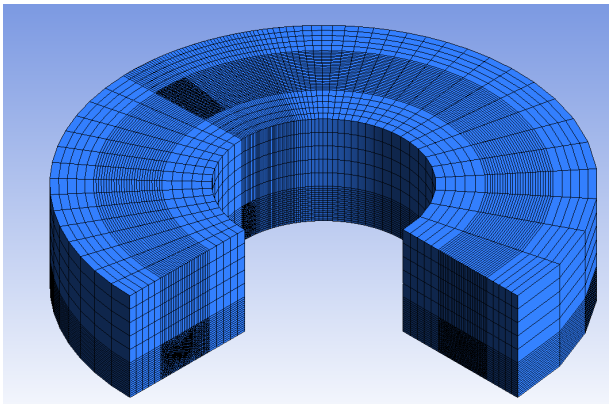

(b) Volume mesh of the wing in the rotating domain

Figure 8: Rotating Domain Mesh

4.4 Set up

The domains were set up using the following parameters. (Table 2)

Parameter	Straight Line Set Up	Rotating Domain Set up
Inlet	40 km/hr	40 km/hr - Theta Component
Outlet	0 Relative Pressure	0 Relative Pressure
Ground	Free Slip Wall	Free Slip Wall
Wall	Free Slip Wall	Free Slip Wall
Rear Wing	No Slip Wall	No Slip Wall
Turbulence Model	k-w SST	k-w SST
Monitor Points	Cl, Cd	Cl, Cd, Cx

Table 2: Domain Set up

The k-w SST turbulence model has been used to capture the boundary layer and according to [3] it has the ability to accurately capture the boundary layer.

The force coefficients were calculated using the following equation:

$$ForceCoefficient = \frac{2 \times Force}{Density \times Velocity^2 \times Area} \tag{1}$$

Where:

Density = 1.225 kg/m^3

Velocity = 11 m/s

Area = 0.3255 m^2

Coefficient of Lift = Cl Coefficient of Drag = Cd Coefficient of Side Force = Cx

4.5 Results

4.5.1 Straight line analysis

The results of the straight line analysis is shown in Table 3. They show a 6% decrease in Cl and a 3% increase in Cd compared to the original design.

End Plate Design	Cl	Cd
Initial Design	2.27	0.75
Modified Design	2.14	0.77
Difference	6%	3%

Table 3: Results from straight line simulation

The pressure contour on the end plate designs are shown in Figure 9. They show that the cut taken from the modified end plate in Figure 9b takes away a portion of the high pressure region. As the bottom section of the end plate has not changed the difference in downforce is due to the reducing of the high pressure region on the top surface.

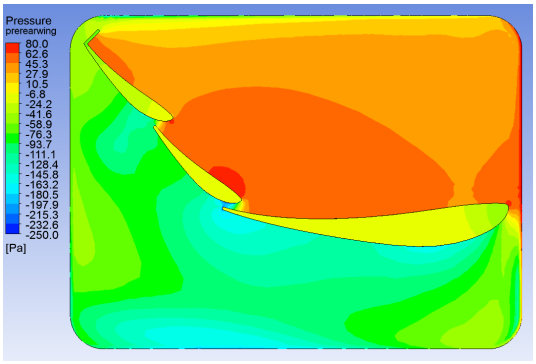

(a) Pressure on Initial Geometry

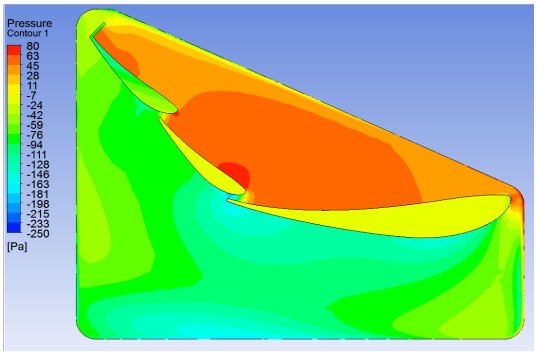

(b) Pressure on Modified Geometry

Figure 9: Pressure on End Plate Design

The flow structure around the end plates create two vorticies at the top and bottom edge. There is a high pressure region on the upper wing surface, pressure is lower on the other side of the end plate creating a clockwise vortex. The opposite can be seen on the bottom side with a counter rotating vortex due to the low pressure region of the profile. The original geometry vortex core can be seen in Figure 10a. The vortex grows down the end plate and expands due to the rotating flow. Figure 10b shows the vortex of the modified end plate, it grows down the end plate and expands but due to the angle of the cut the core grows vertically. As the end plate of the original design is high and further away from the profile, the top vortex does not effect the original design as much.

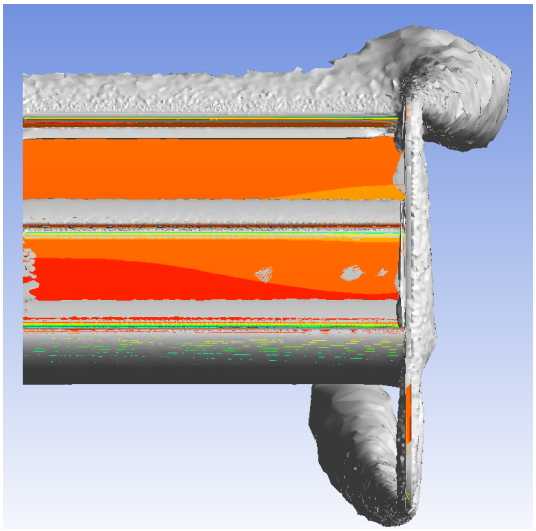

(a) Vortex Core of Initial Geometry

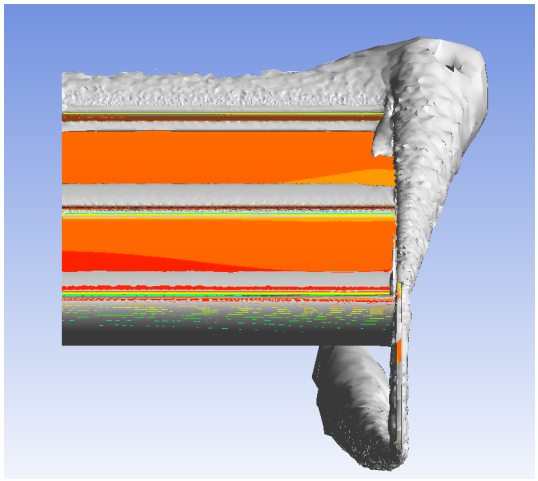

(b) Vortex Core of Modified Geometry

Figure 10: Vortex Core on End Plate Design

The vortex generated by the end plate bleeds pressure from the upper and lower surface of the rear wing, taking a section off the top of the end plate however has a small on the overall Cl and Cd.

4.5.2 Rotating Domain

The results for the Rotating Domain can be seen in Table 4. There is a 1% increase in Cl and no change to Cd of the modified design. As the modified end plate has a smaller area, the force exerted by the air is smaller resulting in a smaller side force. This can be seen in the results as a 20% reduction in side force of the modified design. Compared to the straight line simulations the modified design was more efficient under yaw conditions. The initial geometry reduced Cl by 11% and Cd by 3%. The modified design had a 5% reduction in Cl and 6% in Cd.

End Plate Design	Cl	Cd	Cx
Initial Design	2.03	0.73	0.41
Modified Design	2.01	0.73	0.33
Difference	1%	0%	20%

Table 4: Results from rotating domain simulation

The change in the flow structure changes the pressure exerted by the rear wing changing the force coefficients. The pressure distribution of the lower wing surface is similar, pressure on the upper wing surface show a larger high pressure region of the initial geometry, resulting in more downforce as seen in Figure 11. As the modified end plate is closed to the high pressure region of the profile, the vortex created has a larger low pressure region. This bleeds pressure reducing downforce, accounting for the small reduction in downforce between the two designs.

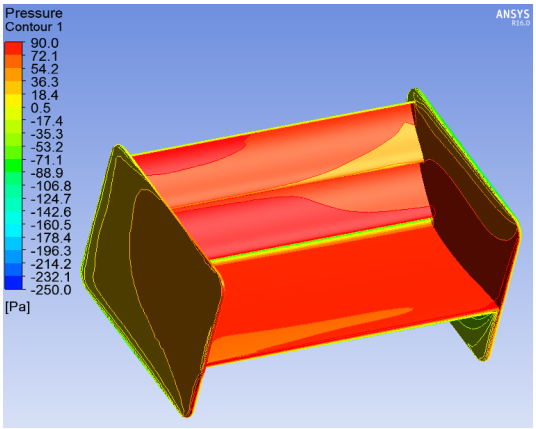

(a) Pressure Contour on Initial Design

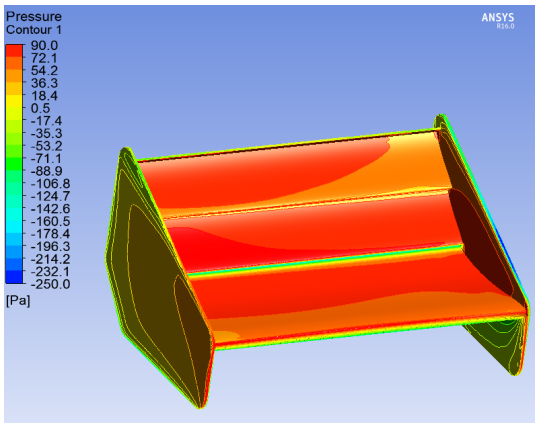

(b) Pressure Contour on Modified Design

Figure 11: Pressure Contour on rear wing

5 Conclusion

The objective of the report was to optimised the end plate design to reduce side force in yaw. A model of the initial design and modified end plate was placed in a straight line and rotating domain.

The straight line analysis created a base line showing the original end plate making 6% more Cl and 3% more Cd. Due to the large end plate the flow was contained with vortexes far away from the profile surface.

The designs were then placed in a rotating domain at a 1.5^0 roll and 10^0 yaw. The results found the modified design making similar Cl and Cd, however saw a 20% reduction in Cx. The report found that the modified geometry was more efficient in yaw.

References

[1] ANSYS. *ANSYS Theory Guide*. 2016

[2] ANSYS. *Meshing User Guide*. 2016

[3] LEAP Australia, *http://www.computationalfluiddynamics.com.au/tips-tricks-turbulence-part-4-reviewing-how-well-you-have-resolved-the-boundary-layer/*. 2013

6 Appendix A

Mesh Type	Number of Elements x10^6	Cl
200 mm volume sizing , 40 mm profile sizing, Inflation: Y+ 1	2.60	1.97
100 mm volume sizing , 20 mm profile sizing, Inflation: Y+ 1	3.34	2.23
50 mm volume sizing , 10 mm profile sizing, Inflation: Y+ 1	3.86	2.23
25 mm volume sizing , 5 mm profile sizing, Inflation: Y+ 1	7.10	2.23

Table 5: Straight and Rotating Domain Dimensions

7 Appendix B

Y+	Number of Elements x10^6	Cl
1	3.34	2.23
7	2.03	2.17
30	1.98	2.22
1.16	1.16	2.22

Table 6: Y+ Study